Journal of the Air & Waste Management Association
Publication details, including instructions for authors and subscription information:
http://www.tandfonline.com/loi/uawm20

Development of regenerative dye impregnated mesoporous silica materials for assessing exposure to ammonia

Yu-Chang Chang [a], Hsunling Bai [a], Hsueh-Shih Chiang [a], Mani Karthik [a], Shou-Nan Li [b], Jung-Nan Hsu [b] & Hui-Ya Shih [b]

[a] Institute of Environmental Engineering, National Chiao Tung University, Hsinchu, Taiwan
[b] Green Energy and Environment Research Laboratories, Industrial Technology Research Institute, Chutung, Hsinchu, Taiwan

Accepted author version posted online: 09 May 2012.Published online: 26 Jun 2012.

To cite this article: Yu-Chang Chang, Hsunling Bai, Hsueh-Shih Chiang, Mani Karthik, Shou-Nan Li, Jung-Nan Hsu & Hui-Ya Shih (2012) Development of regenerative dye impregnated mesoporous silica materials for assessing exposure to ammonia, Journal of the Air & Waste Management Association, 62:7, 838-845, DOI: 10.1080/10962247.2012.683929

To link to this article: http://dx.doi.org/10.1080/10962247.2012.683929

TECHNICAL PAPER

Development of regenerative dye impregnated mesoporous silica materials for assessing exposure to ammonia

Yu-Chang Chang,[1] Hsunling Bai,[1,*] Hsueh-Shih Chiang,[1] Mani Karthik,[1] Shou-Nan Li,[2] Jung-Nan Hsu,[2] and Hui-Ya Shih[2]

[1]*Institute of Environmental Engineering, National Chiao Tung University, Hsinchu, Taiwan*

[2]*Green Energy and Environment Research Laboratories, Industrial Technology Research Institute, Chutung, Hsinchu, Taiwan*

[*]*Please address correspondence to: Hsunling Bai, Institute of Environmental Engineering, National Chiao Tung University, 1001 University Road, Hsinchu, Taiwan; e-mail: hlbai@mail.nctu.edu.tw*

The mesostructured materials MCM-41 and SBA-15 were studied as possible supports of bromocresol green (BG) dye impregnation for the ammonia gas detection because of their large surface area, high regenerative property, and high thermal stability. X-ray diffraction, transmission electron microscopy, scanning electron microscope, and N_2 adsorption analysis were used to characterize the prepared materials. These materials could sense ammonia via visible color change from yellowish-orange to blue color. The color change process of the nanostructured materials was fully reversible during 10 cyclic tests. The results indicated that the ammonia absorption responses of the two nanostructured materials were both very sensitive, and high linear correlation and high precision were achieved. As the gaseous ammonia concentrations were 50 and 5 ppmv, the response times for the SBA-15/BG were only 1 and 5 min, respectively. Moreover, the BG dye-impregnated SBA-15 was less affected by the variation in the relative humidity. It also had faster response for the detection of NH_3, as well as lower manufacturing price as compared to that of the dye-impregnated MCM-41. Such feature enables SBA-15/BG to be a very promising material for the detection of ammonia gas.

Implications: The detector tube is a convenient ambient ammonia detection device. However, almost all the commercial detector tubes can be used once only, which not only increases the purchase cost but also produces lots of waste. In this study, we developed two sensing materials that are sensitive for repeated usage. The two mesoporous silica-based materials, MCM-41 and SBA-15, are impregnated by an organic dye of bromocresol green to induce color change behavior that can be easily observed by the naked eye, and it is concluded that dye-impregnated SBA-15/BG is a very promising material for the detection of ammonia gas.

Introduction

The detection and sensing of ambient ammonia is momentous in concerns of both human beings and other living things. For example, the presence of ammonia in chicken farming can cause eye and respiratory irritation of the stock, which has a negative effect on the egg production. Ammonia affects the health of human beings by irritating eyes, throats, and noses when it reaches the level of 50–100 ppmv (ATSDR, 2004). It can be smelled at a level of higher than 0.04–57 ppmv (NIOSH, 2011). The U.S. National Institute of Occupational Safety and Health (NIOSH) proposes that ammonia should not exceed 25 ppmv over 10 hr per day or 40 hr per week in the workplace. Moreover, the U.S. Occupational Safety and Health Administration (OSHA) has set a limit of 50 ppmv over 8 hr per work day and 40 hr per week for ambient ammonia in air (OSHA, 2011). In order to avoid hazards, there are many studies on ammonia emissions and controls (Blanes-Vidal et al., 2009; Hoff et al., 2006; Lemay et al., 2010; Mukhtar et al., 2009; Ruth 1986; Saha et al., 2010). Fast detection of ambient ammonia gas at a reasonable price has been an important research area with practical concerns.

Passive diffusive sampling systems can be used to accurately monitor ambient ammonia concentrations (Sather et al., 2008; Sun et al., 2008). However, the passive samplers such as the filter pack methods require the adsorption of ammonia onto the filter first, and then the ammonia is extracted and then analyzed by another instrument (Drägerwerk, 2011). Such a process is time-consuming. On the other hand, among all types of direct ammonia gas sensing or detection instruments, the detector tube is one of the popular ammonia detection devices due to its convenience and inexpensive cost. The detector tube is a snapshot sampling device by which the ambient air is drawn through the tube, the ammonia molecules then react with the reagent, and color change occurs. Unlike heavy and expensive optical detection instrument, the detector tubes can be easily carried for the fast detection of ambient ammonia gas at any location with only a small sacrifice in the measurement accuracy ($\pm$10% in standard deviation) (Drägerwerk, 2011). In addition, it is a cheaper device as compared to all other NH_3 measurement instruments. However, commercial detector tubes usually can only be used once and then they have to be discarded.

Journal of the Air & Waste Management Association, 62(7):838–845, 2012. ISSN: 1096-2247 print
DOI: 10.1080/10962247.2012.683929

Several research works reported that porous materials can be good ammonia adsorbents. Amon et al. (1997) and Kelleher et al. (2002) used the commercial clinoptilolite zeolite coating on building material to remove ammonia and odor in the livestock industry. Critoph (2002) tested the ammonia gas adsorption and desorption via the use of porous activated carbon and proved that this had good ammonia removal efficiency and could be reused by desorption. These studies provide a clue that reusable ammonia detection materials can be fabricated using the porous material as a matrix to produce chemosensing reagents. More recently, ordered mesoporous silica materials are of interest for several applications, due to uniform nanoporosity, mechanical stiffness, thermal stability, high surface area and pore volume, tunable pore size, and the possibility of incorporation of heteroatoms into the silica structure (Kosslick et al., 1999; Kresge et al., 1992; Matsumoto et al., 1999). The nonflammable porous silica-based material is better than the flammable carbon-based material when safety is of concern.

Some studies had shown that mesoporous silica-based material could be ammonia-sensing material. Onida et al.- (2004) used mesoporous SBA-3 that was impregnated with Reichardt's dye to develop an ammonia sensor and the results showed that the response time was 27 sec when exposing to 1000 ppmv ammonia. Fiorilli et al.- (2004) used mesoporous SBA-15 impregnated with Reichardt's dye to fabricate an ammonia sensor and proved that the sensing process was fully reversible in 1% ammonia concentration. Wark et al.- (2003) used mesoporous siliceous MCM-41 with SnO_2 as the ammonia-sensing material. By using ultraviolet–visible (UV-Vis) spectroscopy, it could detect ammonia gas at the concentration of 50 ppmv. However, the degree of the color change could not be easily sensed by naked eyes. For the sensing materials used in the detector tube, the observable difference in terms of color change is essential. And to the authors' knowledge, reusable ammonia detection material that can detect at the concentration range of low ppmv levels (<50 ppmv) has not been developed as a detector tube.

Two mesoporous silica-based materials, MCM-41 and SBA-15, are discussed in this study. They possess the unique properties of uniform nanoporosity, large surface area, high regenerative ability and high thermal stability (Kosslick et al., 1999; Kresge et al., 1992; Matsumoto et al., 1999). These two materials are sensitive upon exposure to the ammonia gas-containing environment (Fiorlli et al., 2004; Wark et al., 2003). The materials of MCM-41 and SBA-15 are impregnated by an organic dye of bromocresol green (BG) to induce the color change behavior. The organic compound is originally in yellowish-orange color, and turns to blue color when it reacts with ammonia gas. These two materials are compared by their response time under different conditions of relative humidity, ammonia inlet concentrations, and reversibility.

Experimental

Preparation of Mesoporous MCM-41

Cetyl-trimethylammonium bromide (CTABr, $C_{19}H_{42}BrN$) was used as a surfactant template. MCM-41 samples were synthesized from gels with the following molar composition: 1 Na_2SiO_3, 0.2 CTABr, 0.8 H_2SO_4, 96.8 H_2O. The typical synthesis procedure for MCM-41 was performed as follows: 21.2 g of sodium metasilicate (Kanto Chemical Co., Inc., Japan) and 80 ml of deionized water were mixed and stirred for 30 min. Then, 11.1 ml H_2SO_4 (Panreac Chemicals Co., Spain) in 100 ml of deionized water was slowly added to the mixture to bring down the pH to 10.52 under constant stirring to form a gel. After stirring, 7.2 g of CTABr (Merck & Co. Inc., Germany) in 25 ml deionized water was added slowly into the preceding mixture and the combined mixture was stirred for 3 additional hours. The resulting gel mixture was transferred into a Teflon-coated autoclave and kept in an oven at 145°C for 36 hr. After cooling to room temperature, the resultant solid was recovered by filtration, washed with distilled water, and dried in an oven at 100°C for 6 hr. The organic template was removed using a muffle furnace in air at 550°C for 6 hr. Finally, the material was milled to achieve a minimum size range. The powder form of the porous material was in the size range of around 0.1–1 μm; thus, it should be used in caution since it might be inhaled into the respiratory system.

Preparation of Mesoporous SBA-15

Polyethylene glycol (P123, $EO_{20}PO_{70}EO_{20}$, Mn5800, Aldrich, Germany) was used as the surfactant template. The molar composition of the gel was 1 SiO_2, 0.01 P123, 0.18 H_2SO_4, 210 H_2O. For surfactant solution, 2 g of P123 surfactant was dissolved into 50 ml distilled water and stirred for 1 hr under 40°C. Meanwhile, 8 g of sodium silicate ($Na_2Si_3O_7$, Sigma-Aldrich, Germany) was added into 50 mL distilled water and stirred for 20 min. Then, 26 mL of 0.23 *M* H_2SO_4 (Merck, Germany) was added into the sodium silicate solution until the pH value became 2.0. Then 6 *M* of NaOH (Fisons, England) solution was added drop by drop into the sodium silicate solution to adjust the pH to 5.0 under vigorous stirring. The surfactant solution was then added into the sodium silicate solution and stirred for 3 min. The resulting gel was transferred into an autoclave and kept in an oven at 100°C for 24 hr. After cooling to room temperature, the resultant solid was recovered by filtration, washed with deionized water, and dried in an oven at 60°C for 24 hr. The materials were calcined in a muffle furnace at 500°C for 6 hr. Finally, the material was milled to achieve a minimum size range.

Impregnation of Bromocresol Green Indicator

The bromocresol green dye (BG) is a weak organic acid whose absorbance spectrum is quite different from the absorbance spectrum of its conjugate base. A bromocresol green solution changes its color from yellow to blue over the pH range of 3.8–5.4 (Ibarra et al., 2004). The dye impregnating procedure was performed as follows: 0.001 g of bromocresol green powder (Acros Organics Co., USA) and 100 mL of acetone (Merck & Co., Inc., Germany) were mixed and stirred for 10 min. Then 0.1 g of MCM-41 or SBA-15 powder was added and stirred for another 3 hr. The resulting yellow solution was transferred into an evaporating dish and kept in an explosion-proof oven at 110°C for 4 hr. Finally the orange-colored powders of BG dyeimpregnated MCM-41 and SBA-15 materials were

collected and are named as MCM-41/BG and SBA-15/BG hereafter.

Characterization

The powder x-ray diffraction patterns of MCM-41 and MCM-41/BG samples were recorded using a Panalytical X'Pert Pro MRD powder diffractometer, where Cu target Kα-ray (operating at 30 kV and 20 mA) was used as the x-ray source. The scanning range was $2\theta = 2^\circ$ to 10° with the rate of 1.2°/min, and the *d*-spacing (d_{hkl}) of materials was calculated by the Bragg law (Peura, 2007). The powder x-ray diffraction patterns of SBA-15 and SBA-15/BG samples were also recorded and the scanning range was $2\theta = 0.3^\circ$ to 5° with a rate of 0.02°/min.

The N_2 adsorption/desorption analysis was carried out on a Micromeritics ASAP 2020 at 77 K. The samples were degassed at 350°C before measurements. The surface area was obtained by the Brunauer–Emmett–Teller (BET) method (Satterfield, 1993) and the pore size distribution was calculated from the adsorption branch of isotherm using the Barrett–Joyner–Halenda (BJH) method.

Transmission electron microscopy (TEM; JEOL JEM 1210, Japan) was carried out on a JEOL JEM-2010 microscope at 120 kV. The specimens for TEM were prepared by epoxy resin imbedded microsection and mounting on copper grid. The morphology of MCM-41 and SBA-15 was examined by scanning electron microscope (Hitachi, S4700, Japan).

Ammonia Gas Detection

In order to test the performance of the dye-impregnated mesoporous materials on ammonia gas detection, the set-up of experimental detector tube is schematically shown in Figure 1. The detector tube was made from glass with an inner diameter of 5 mm, which is a typical size used in some commercial detector tubes. A sponge was used as the support for the dye-impregnated mesoporous materials in the glass tube. Because powder materials are not suitable for the detector tube since they would induce high pressure drop, the powder materials were pelletized, broken into small pieces, and then sieved with the 16 to 30 mesh to obtain a proper size range for the ammonia detection purpose. The packed depth of the dye-impregnated mesoporous materials was 3 cm.

The inlet ammonia gas concentration was supplied by a gas cylinder and was measured by an NH_3 analyzer using the SIR model-S5012 (Spain) (SIR, 2011) with a catalytic converter. The NH_3 gas was diluted with clean and compressed air to produce ppmv levels of ammonia concentration. All the gas flow rates were controlled by mass flow controllers (MKS, 1179A, USA), which were calibrated by a bubble meter before every test. The total flow rate of diluted ammonia gas was 1000 mL min^{-1}, which was selected due to its fast response times of a few minutes for the tested range of NH_3 concentration, 5–50 ppmv. The temperature of this test system was at room temperature (24 ± 1°C). The relative humidity (RH), monitored by a humidity and temperature meter (Center 310, JDC Electronic SA, Switzerland), can be adjusted by the use of two water impingers, and it was 50 ± 5% or 80 ± 5% RH during the experiment to represent the typical RH range for a majority of cities around the world.

When the ammonia gas flow was passed through the detector tube, a color change from yellow to blue occurred and the depth of color change increased horizontally downward with time. The comparison of the two materials was done by the time required to achieve observable color change of 1 cm. For the tests on cyclic ability, a desorption process was done by heating the detection tube at 120°C for 1 hr.

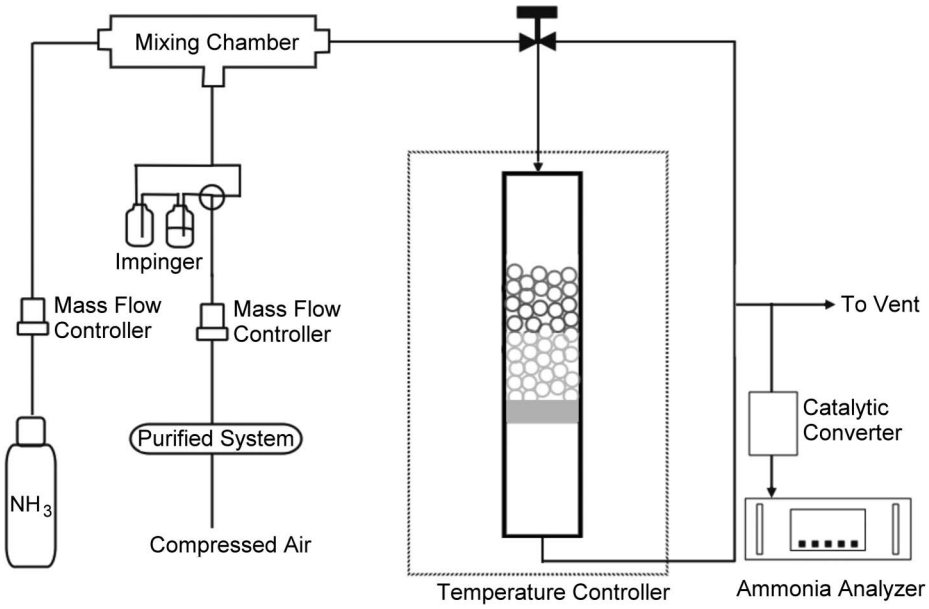

Figure 1. Schematic diagram of a laboratory set-up for NH_3 gas detection via a detector tube.

Results and Discussion

Material Characterization

The XRD patterns of MCM-41and dye impregnated MCM-41/BG are shown in Figure 2a, while the XRD patterns of SBA-15 and dye impregnated SBA-15/BG are shown in Figure 2b. The MCM-41 material shows the characteristic reflection of mesoporous structure. Besides the strong peak at (100), weak peaks at (110) and (200) reflections were also observed even after dye impregnation. This means the dye impregnation process did not affect the order of porous structure. The XRD patterns of SBA-15 and SBA-15/BG showed a significant peak at around 0.75°, suggesting a mesoporous structure was also observed for SBA-15. However the broad peak indicates low uniformity of pore distribution. The interplanar spacings (d_{100}) of MCM-41 and SBA-15 are listed in Table 1. The value of d_{100} for MCM-41 was 4.01 nm, and it was 11.76 nm for SBA-15. Similar d_{100} of 3.94 nm and 11.45 nm were observed for MCM-41/BG and SBA-15/BG samples, respectively, which indicates that the dye molecules did not affect the order of porous structure.

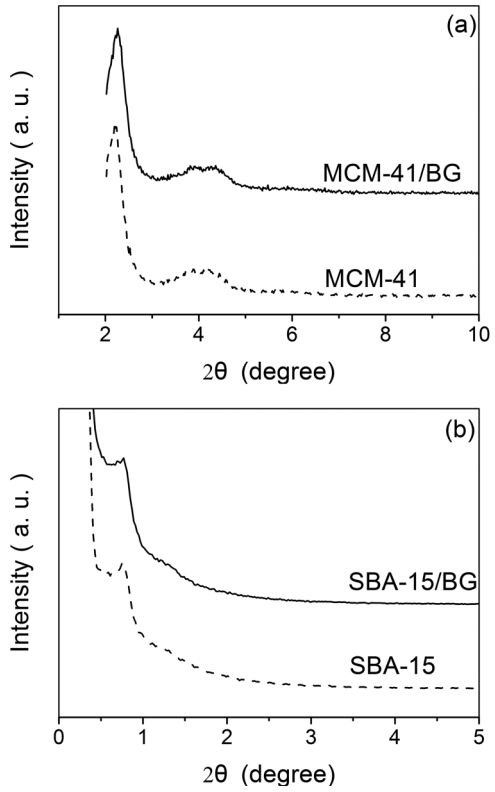

Figure 2. Powder X-ray diffraction patterns. (a) MCM-41 and dye-impregnated MCM-41/BG (b) SBA-15 and dye-impregnated SBA-15/BG.

The N_2 adsorption/desorption analyses were performed for the MCM-41 and SBA-15 materials; however, one could not perform the N_2 adsorption/desorption analyses for the dye-impregnated samples because of the volatile property of the BG dye, which could damage the instrument. The results for the N_2 adsorption/desorption isotherms of MCM-41 and SBA-15 are shown in Figure 3. Both isotherms were type IV according to IUPAC classification (Rouquerol et al., 1994), and the uptake of N_2 due to capillary condensation was observed at relative pressure (p/p_0) ranges of 0.3–0.4 and 0.6–0.9, respectively, for MCM-41 and SBA-15. Such isotherms were characteristics of mesoporous materials with transitional pore sizes from microporous to mesoporous materials.

Results on the physical characterization of the MCM-41 and SBA-15 materials are listed in Table 1. The BET surface areas were 1079 m^2/g and 460 m^2/g, respectively, for MCM-41 and SBA-15. And Figure 4 shows the pore size distributions of MCM-41and SBA-15. The MCM-41 showed a narrow pore size distribution with mode diameter at 2.70 nm. Such mode diameter was close to the BJH average pore diameter of 3.2 nm shown in Table 1. However, the pore size of SBA-15 appeared to be bimodally distributed, with one mode size at around 4.7 nm and the other mode size at 9.3 nm. The BJH average pore size of the SBA-15 was 8.1 nm.

The scanning electron microscope (SEM) images of the MCM-41 and SBA-15 are shown in Figure 5a and Figure 5b, respectively. The MCM-41 materials were in either tube or irregular particle shapes with particle diameter of ~100 nm as roughly measured from the SEM images. The particle size of the SBA-15 was also similar to that of the MCM-41 if particles were not agglomerated. However, once the SBA-15 particles were aggregated, their particle size could be larger than that of MCM-41.

The transmission electron microscopy (TEM) images of MCM-41, MCM-41/BG, SBA-15, and SBA-15/BG are shown in Figure 6. The TEM image of MCM-41 confirmed the ordered hexagonal structure, and the hexagonal pore structure of dye impregnated MCM-41/BG was still observable by the TEM image. The TEM images of SBA-15 and SBA-15/BG showed less uniformity in their pore size distribution as compared to those of MCM-41 and MCM-41/BG. The clear observation of the pores for both MCM-41/BG and SBA-15/BG indicates that

Table 1. Physical characterization properties of MCM-41 and SBA-15

Sample name	S_{BET} [a] (m^2/g)	V_p [b] (cm^3/g)	d_{BJH} [c] (nm)	Mode diameter (nm)	d_{100} [d] (nm)	a, Unit cell [e] (nm)
MCM-41	1079	1.00	3.2	2.7	4.0	4.6
SBA-15	460	0.85	8.1	4.7, 9.3	11.8	13.6

Notes: [a]BET surface area. [b]Pore volume. [c]Pore diameter calculated by BJH theory. [d]d-Spacing between (1 0 0) planes. Calculated from $2d \sin\theta = n\lambda$. [e]Hexagonal unit cell. Calculated from $a = 2d_{100}/\sqrt{3}$.

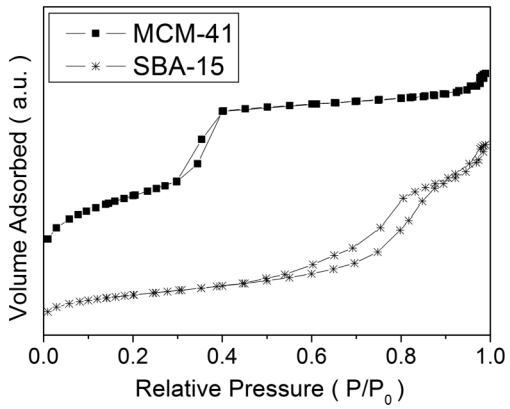

Figure 3. N_2 adsorption/desorption isotherms of MCM-41 and SBA-15.

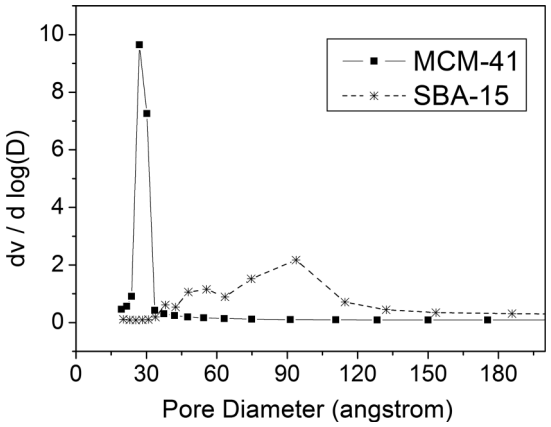

Figure 4. BJH pore size distributions of MCM-41 and SBA-15.

the dye molecules didn't block the nanopore structure of the host materials.

Ammonia Gas Detection

When a gas sample containing ammonia gas was brought into contact with the dye-impregnated materials, ammonia molecules in the gas sample diffuse into the porous materials and react with the BG dye. This reaction reduces the concentration of BG and increases the concentration of BG salt. Similar to most pH indicators, BG dye is a weak organic acid whose absorbance spectrum is quite different from that of its conjugate base (Oberg et al., 2006). The color of BG solution changes from yellow to blue over the pH range of 3.8–5.4, and it indicates the equilibrium shifts to the deprotonated, arylmethine form of the dye (Wang and Sun, 1987). Bromocresol green was selected based on the comparison of three candidate dyes (Markovics et al., 2009) for ammonia detection: bromophenol blue (BPB), bromocresol green (BG), and bromocresol purple (BCP). The respective pK_a values are 3.8 for BPB, 4.7 for BG, and 6.0 for BCP. A lower pK_a value of the dye indicates faster response time. However, the decrease in the pK_a value of the dye also results in a longer desorption time. Thus BG should offer an appropriate compromise between the needs for fast response and fast desorption (Markovics et al., 2009).

The response times for observable color change of MCM-41/BG and SBA-15/BG were only around 5 sec. However, to simulate the performance of a commercialized detector tube, which is evaluated based on the color change over a certain depth, the following results are presented based on the response time of per 1-cm change in color from yellow to blue in the detector tube at a flow rate of 1000 mL min^{-1}.

Because ammonia is easily dissolved in water, the relative humidity effect is always an important parameter for ammonia sensors. Figure 7 compares the effect of relative humidity on the ammonia detection with SBA-15/BG and MCM-41/BG. In total, three repeated tests were performed and the average response times with error bars are shown in Figure 7. The color change time of SBA-15/BG was faster than that of MCM-41/BG. The longer response time of the MCM-41/BG could be due to the larger surface area, which was capable of adsorbing more ammonia molecules, so that its ammonia saturated capacity was larger and the color change process became longer. The response time for MCM-41/BG was strongly affected by the relative humidity (RH). At RH of 50% the average response time was 390 sec, but it increased to 620 sec at RH of 80%. For the SBA-15/BG material, the response time was almost the same at around 250 sec for 50% and 80% RH. This is because that the prepared SBA-15 has a higher hydrophobic property as compared to the MCM-

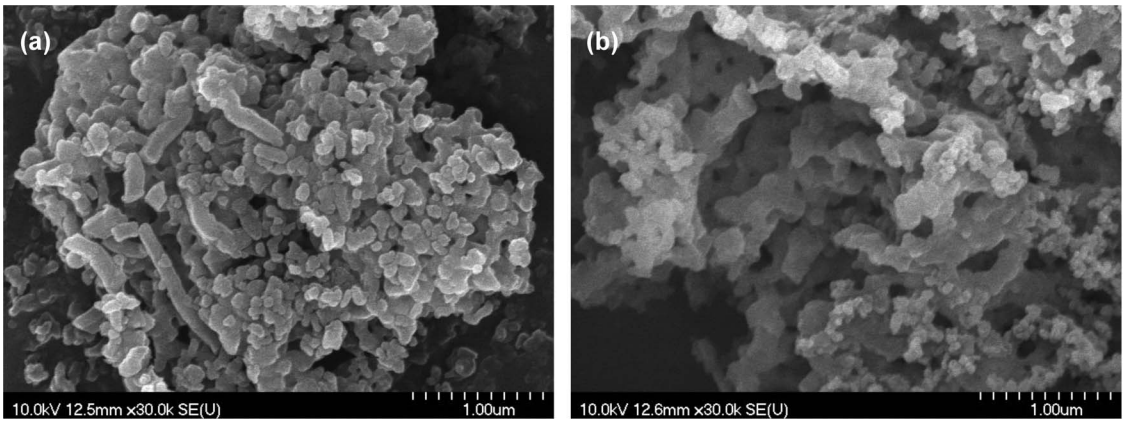

Figure 5. Scanning electron microscope images of (a) MCM-41 and (b) SBA-15.

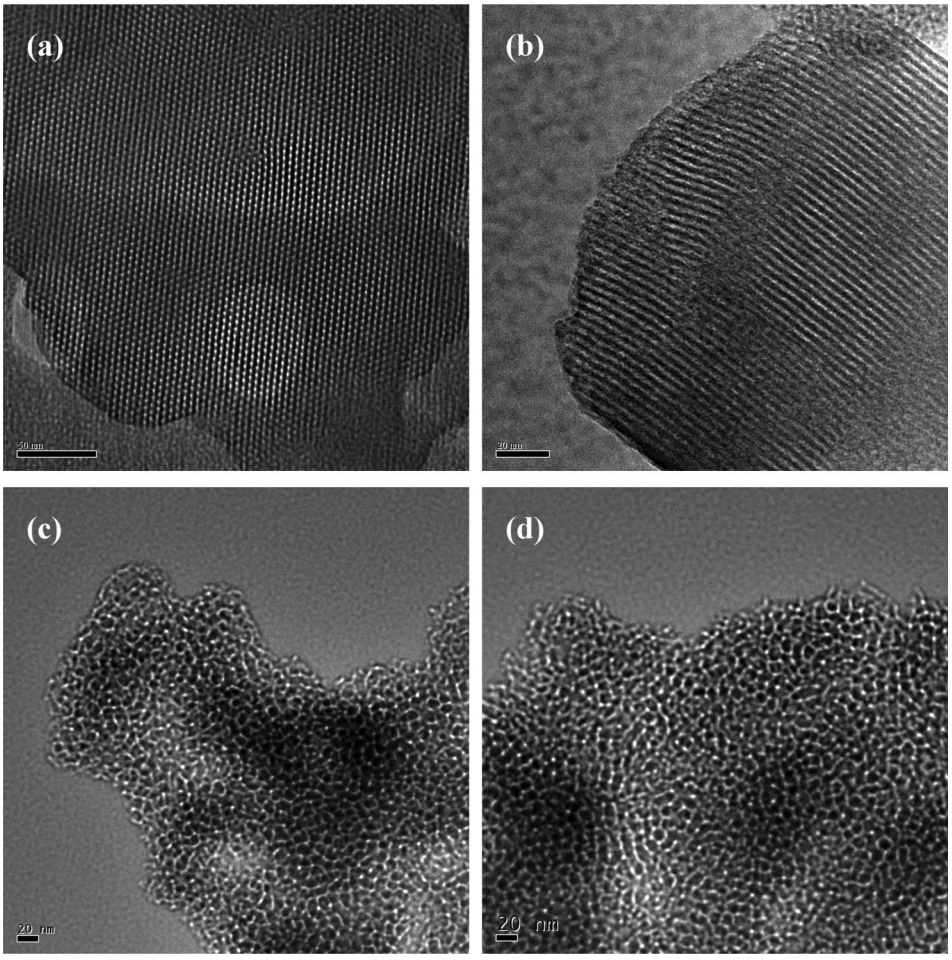

Figure 6. Transmission electron micrographs of (a) MCM-41, (b) Dye-impregnated MCM-41/BG, (c) SBA-15, and (d) dye-impregnated SBA-15/BG. The scale bars for all images are 20 nm except for (a), where the scale bar is 50 nm.

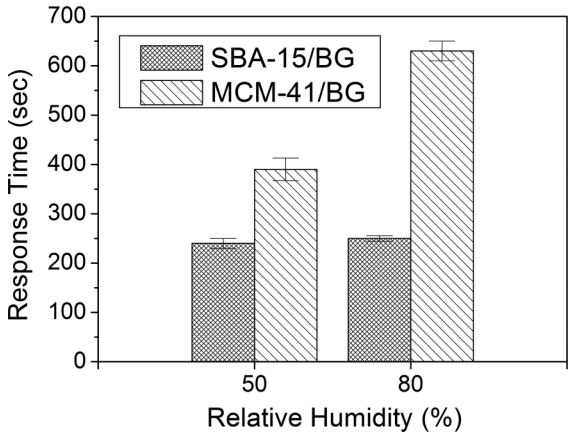

Figure 7. The effect of relative humidity on the response time of dye impregnated materials of MCM-41/BG and SBA-15/BG. The response time was defined by per 1 cm change in color from yellow to blue in the detector tube at a flow rate of 1000 ml min^{-1}. The inlet ammonia concentration was 10 ppmv and the temperature was 25°C.

41. For the MCM-41 material, the moisture could be competitively adsorbed with the ammonia at higher values of relative humidity. Based on the relative humidity tests, it seems that the SBA-15/BG is a more suitable material as a dye-supporting material for the detection of ammonia gas. The SBA-15/BG not only can detect ammonia gas at a faster rate, but also is less affected by the presence of moisture.

To explore the effect of inlet ammonia gas concentration on the response time of the ammonia detection, tests were performed on the ammonia gas inlet concentration of 5 to 50 ppmv. This concentration range is critical for meeting the standard limits set by the NIOSH and OSHA. Figure 8 shows the linear correlation results at this concentration range for MCM-41/BG and SBA-15/BG. One can see that high linear correlation coefficients were obtained under the test concentration range of 5–50 ppmv. For the regression lines shown in Figure 8, the 95% confidence limits for the slope of MCM-41/BG and SBA-15/BG on ammonia detection are -8.167 ± 1.873 and -5.267 ± 1.998, respectively. And the 95% confidence limits for the intercept of MCM-41/BG and SBA-15/BG are 484.17 ± 56.96 and 304.67 ± 60.76, respectively. The correlation coefficients (R^2) are 0.9847 for MCM-41/BG and 0.9591 for SBA-15/BG, respectively. Although this value cannot meet the analytical requirement ($R^2 > 0.990$), as a standard method of sampling and analysis, this is good enough as a low-cost detector for in situ measurement of industrial or agriculture emission of ammonia

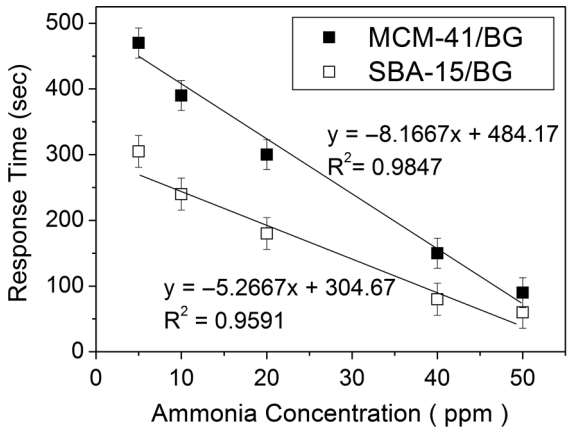

Figure 8. The effect of ammonia concentration on the response time of dye impregnated materials in the detector tube. The relative humidity was 50%. The response time was defined by per 1 cm change in color from yellow to blue in the detector tube at a flow rate of 1000 mL min^{-1}.

gas. The color change time became shorter as the ammonia gas concentration was higher. In addition, the time difference between MCM-41/BG and SBA-15/BG became smaller as the ammonia concentration was higher. At an ammonia gas concentration of 50 ppmv, the detection times required to have 1 cm color change were 90 and 60 sec, respectively, for MCM-41/BG and SBA-15/BG.

The reversibility of the MCM-41/BG and SBA-15/BG materials for ammonia gas detection was tested for 10 cyclic times by repeated adsorption/desorption at an inlet ammonia concentration of 10 ppmv. The results of 10 cyclic tests are shown in Figure 9. The required color change time for SBA-15/BG was 249 ± 9 sec (3.8% in relative standard deviation [RSD]), and for MCM-41/BG it was 636 ± 18 sec (2.9% in RSD). The results proved that both MCM-41/BG and SBA-15/BG showed good reproducibility data and are reliable for repeated usage as color change materials in the detector tube. Similar tests were also performed for coating BG on non-mesoporous materials such as silica gel and Al_2O_3, as well as for some of the commercial detection tube products. The results reveal that they show poor performance in detecting ammonia gas, and none of them show regenerative properties.

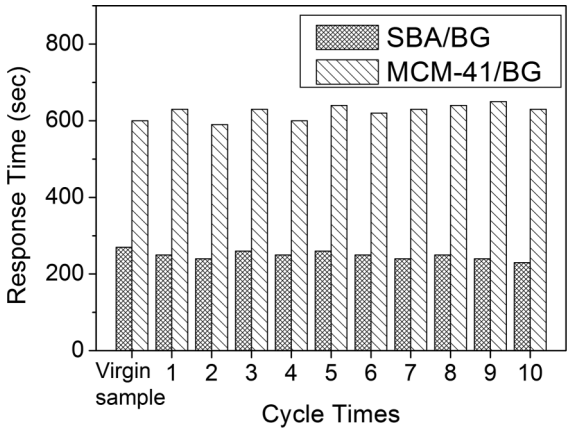

Figure 9. Reversibility tests of the dye impregnated materials. The inlet ammonia concentration was 10 ppmv and the relative humidity was 80%. The response time was defined by per 1 cm change in color from yellow to blue in the detector tube at a flow rate of 1000 mL min^{-1}.

Conclusions

Sensitive and fully reversible dye materials of MCM-41/BG and SBA-15/BG have been prepared and demonstrated to be suitable materials for detector tubes on ammonia gas detection. The organic BG dye compound supported on the MCM-41 and SBA-15 mesoporous materials was originally yellowish-orange color, and turned to blue color when reacted with ammonia gas. Based on the results in this study, it was concluded that dye-impregnated SBA-15/BG was less affected by relative humidity, and shows faster response time of around 1 to 5 min for detecting 5 to 50 ppmv of ammonia gas. Thus, SBA-15/BG is better in performance than MCM-41/BG. Besides, the reagent-grade chemical cost of SBA-15/BG (∼US$0.16/g) was only about one-fifth of that of the MCM-41/BG (∼US$0.79/g). The chemical price of the SBA-15/BG material is only one-fiftieth of the price of commercial detector tubes (which cost around US$8.00–10.00/tube in Taiwan); the price of SBA-15/BG could be even much lower when considering repeated usage. This enables SBA-15/BG to be the prominent sensing material for industrial application. Future work should be performed on possible interferences with the ammonia detection, such as from other amine species.

Acknowledgment

The authors from Industrial Technology Research Institute thank the Department of Industrial Technology (DoIT), Ministry of Economic Affairs (MOEA) in Taiwan for sponsoring this study.

References

Agency for Toxic Substances & Disease Registry. 2004. Toxicological Profile for Ammonia. http://www.atsdr.cdc.gov (accessed February 20, 2012).

Amon, M., M. Dobeic, R.W. Sneath, V.R. Phillips, T.H. Misselbrook, and B.F. Pain. 1997. A farm-scale study on the use of chinoptilolite zeolite and deodorase for reducing odour and ammonia emissions from broiler houses. *Bioresource Technol.* 61:229–237.

Blanes-Vidal, V., S.G. Sommer, and E.S. Nadimi. 2009. Modelling surface pH and emissions of hydrogen sulphide, ammonia, acetic acid and carbon dioxide from a pig waste lagoon. *Biosystems Eng.* 104:510–521.

Critoph, R.E. 2002. Multiple bed regenerative adsorption cycle using the monolithic carbon-ammonia pair. *Appl. Therm. Eng.* 22:667–677.

Drägerwerk AG & Co. 2011. Introduction of the detector tube, ammonia 2/a. http://www.draeger.com (accessed February 22, 2012)

Fiorilli, S., B. Onida, D. Macquarrie, and E. Garrone. 2004. Mesoporous SBA-15 silica impregnated with Reichardt's dye: A material optically responding to NH_3. *Sensors Actuators B* 100:103–106.

Hoff, S.J., D.S. Bundy, M.A. Nelson, B.C. Zelle, L.D. Jacobson, A.J. Heber, J. Ni, Y. Zhang, J.A. Koziel, and D.B. Beasley. 2006. Emissions of ammonia, hydrogen sulfide, and odor before, during, and after slurry removal from a deep-pit swine finisher. *J. Air Waste Manage. Assoc.* 56:581–590.

Ibarra, J.C., M. Ortiz-Gutierrez, and P. Alonso-Magana. 2004. Characterization of bromocresol green and resin as holographic film. *Optical Mater.* 27:567–572.

Kelleher, B.P., J.J. Leahy, A.M. Henihan, T.F. O'Dwyer, D. Dutton, and M.J. Leahy. 2002. Advances in poultry litter disposal technology, a review. *Bioresource Technol.* 83:27–36.

Kosslick, H., G. Lischke, B. Parlitz, W. Storek, and R. Fricke. 1999. Acidity and active sites of Al-MCM-41. *Appl. Catal. A.* 184:49–60.

Kresge, C.T., M.E. Leonowicz, W.J. Roth, J.C. Vartuli, and J.S. Beck. 1992. Ordered mesoporous molecular-sieves synthesized by a liquid-crystal template mechanism. *Nature* 359:710–712.

Lemay, S.P., L. Chenard, H.W. Gonyou, J.J.R. Feddes, and E.M. Barber. 2010. A two-airspace building design to reduce odor and ammonia emissions. *Appl. Eng. Agric.* 26:649–658.

Markovics, A., G. Nagy, and B. Kovacsa. 2009. Reflection-based sensor for gaseous ammonia. *Sensors and Actuators B* 139:252–257.

Matsumoto, A., H. Chen, K. Tsutsumi, M. Grun, and K. Unger. 1999. Novel route in the synthesis of MCM-41 containing framework aluminum and its characterization. *Microporous Mesoporous Mater.* 32:55–62.

Mukhtar, S., A. Mutlu, R.E. Lacey, and C.B. Parnell. 2009. Seasonal ammonia emissions from a free-stall dairy in central Texas. *J. Air Waste Manage. Assoc.* 59:613–618. doi:10.3155/1047-3289.59.5.513

National Institute of Occupational Safety and Health. 2011. http://www.cdc.gov/niosh (accessed February 20, 2012).

Oberg, K.I., R. Hodyss, and J.L. Beauchamp. 2006. Simple optical sensor for amine vapors based on dyed silica microspheres. *Sensors Actuators B* 115:79–85.

Occupational Safety and Health Administration (OSHA), US. 2011. http://www.osha.gov (accessed February 21, 2012).

Onida, B., L. Borello, S. Fiorilli, B. Bonelli, C.O. Arean, and E. Garrone. 2004. Mesostructured SBA-3 silica containing Reichardt's dye as an optical ammonia sensor. *Chem. commun.* 21:2496–2497.

Peura, M. 2007. *Studies on the Cell Wall Structure and the Mechanical Properties of Norway Spruce*, p. 15. Helsinki: Helsinki University Printing House.

Rouquerol, J., D. Avnir, C.W. Fairbridge, D.H. Everett, J.H. Haynes, N. Pernicone, J.D.F. Ramsay, K.S.W. Sing, and K.K. Unger. 1994. Recommendations for the characterization of porous solids. *Pure Appl. Chem.* 66:1739–1758.

Ruth, J.H. 1986. Odor thresholds and irritation levels of several chemical substances: A review. *Am. Ind. Hyg. Assoc. J.* 47:A142–151.

Saha, C.K., G. Zhang, P. Kai, and B. Bjerg. 2010. Effects of a partial pit ventilation system on indoor air quality and ammonia emission from a fattening pig room. *Biosystems Eng.* 105:279–287.

Sather, M.E., J. Mathew, N. Nguyen, J. Lay, G. Golod, R. Vet, J. Cotie, T. Hertel, E. Aaboe, R. Callison, J. Adam, D. Keese, J. Freise, A. Hathcoat, B. Sakizzie, M. King, C. Lee, S. Oliva, G.S. Miguel, L. Crow, and F. Geasland. 2008. Baseline ambient gaseous ammonia concentrations in the four corners area and eastern Oklahoma, USA. *J. Environ. Monit.* 10:1319–1325.

Satterfield, C.N. 1991. *Heterogeneous Catalysis in Industrial Practice*, 2nd ed., 131–174. New York, NY: McGraw-Hill.

SIR. 2011. Introduction of the NH_3 analyzer. SIR website, Spain. http://www.sirsa.es/english/measurement_instrumentation/air/nox_analyzer.htm (accessed November 30, 2011).

Sun, G., H. Guo, J. Peterson, B. Predicala, and C. Lague. 2008. Diurnal odor, ammonia, hydrogen sulfide, and carbon dioxide emission profiles of confined swine rower/finisher rooms. *J. Air Waste Manage. Assoc.* 58:1434–1448. doi:10.3155/1047-3289.58.11.1434

Wang, E., and Z.S. Sun. 1987. Ion transfer of bromocresol green across liquid–liquid interfaces. *Anal. Chem.* 59:1414–1417.

Wark, M., Y. Rohlfing, Y. Altindag, and H. Wellmann. 2003. Optical gas sensing by semiconductor nanoparticles or organic dye molecules hosted in the pores of mesoporous siliceous MCM-41. *Phys. Chem. Chem. Phys.* 5:5188–5194.

About the Authors

Yu-Chang Chang and **Hsueh-Shih Chiang** obtained their master's degrees from the Institute of Environmental Engineering, National Chiao Tung University (NCTU), Taiwan. **Dr. Hsunling Bai** is a professor and **Dr. Mani Karthik** is a postdoctorate at the Institute of Environmental Engineering, NCTU.

Dr. Shou-Nan Li, **Dr. Jung-Nan Hsu**, and **Hui-Ya Shih** work for the Industrial Technology and Research Institute, Taiwan.